Insight into Astrophysical Phenomena from VLBI Source Position Instabilities

César Gattano, Patrick Charlot

Abstract Most of the radio sources observed by VLBI, some used as defining sources in the International Celestial Reference Frame [ICRF2], show instabilities in position. These instabilities may be caused by astrophysical phenomena occurring in the central VLBI region of these objects (i.e., active galactic nuclei). On this basis, we have begun to characterize the signal included in the available VLBI position time series. Often, position instabilities happen along a preferred direction. There are cases, however, where two directions are distinguishable. The first scenario is consistent with a regular emergence of jet components from the VLBI core; hence, causing shifts of the radio emission centroid. On the other hand, the second scenario may give clues to the presence of a second black hole within the system that has its own activity offset from that of the first black hole. Comparing these directions with the orientation derived from radio-optical position offset brings further insights into astrophysical phenomena within active galactic nuclei.

Keywords Astrometry, celestial frame, source stability

1 Introduction

Active Galactic Nuclei [AGN] are currently the most appropriate sources in the Universe to define stable fiducial marks on the celestial sphere. The reason is that they show no apparent proper motion due to their extragalactic distance from us.

Laboratoire d'Astrophysique de Bordeaux, Université de Bordeaux, OASU, CNRS

However, when we have a look at their position evolution, we often note astrometric instabilities, i.e., systematic variations regarding the measurement uncertainty (see Section 3). Such instabilities vary from source to source, generally in the range 0.1–1 mas and characterize the astrometric behavior of the source. A recent study [3] revealed that among the most observed sources with VLBI, only 5% have a stable astrometric behavior and this fraction cannot be increased much even if loosening the criteria that define stability.

This variability may have two origins. First, it may be an effect of the observing system (i.e., extrinsic to the source) imperfectly taken into account during the data reduction. On the other hand, VLBI, due to its resolving power, is sensitive to the source apparent structure despite their cosmic distances. Indeed, at the milliarcsecond resolution, sources are not point-like, neither do they present a symmetric structure in radio. The photometric variability, sometimes correlated with the astrometric variability, provides hints in favor of source intrinsic effects [13]. The interest in astro-geodesy is to observe sources with the least astrometric variability. Our study aims to extract and collect information that may help to identify these appropriate sources.

2 Preliminary Global Analysis

First, we searched for source astrophysical and observational parameters that may discriminate between sources with stable or unstable observed behavior. We used the VLBI source classification of Gattano et al. [3], built by using the Allan standard deviation to characterize the source behavior. It is divided into three categories: AV0 (stable), AV1 (intermediate),

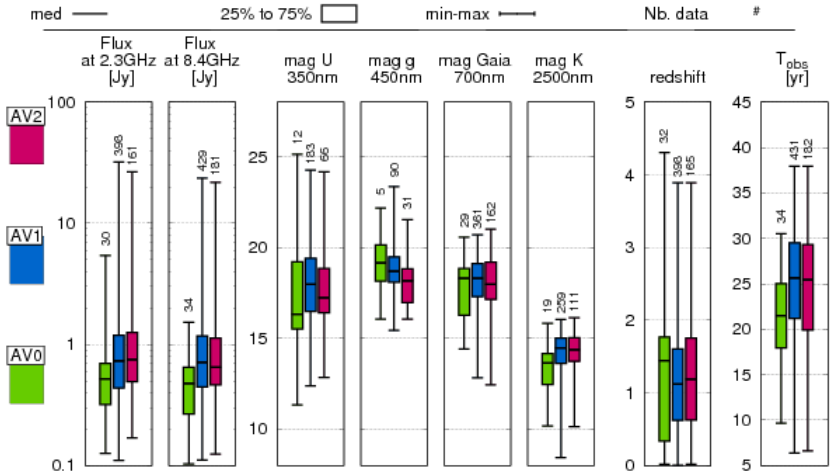

Fig. 1 Distribution of 647 well observed VLBI sources considering the Gattano et al. [3] source classification and regarding several source parameters independently. AV0 sources (green) are sources presenting a stable astrometric behavior, whereas AV2 sources (red) present an unstable astrometric behavior. AV1 sources (blue) are intermediate. Each candlestick gives, from bottom to top, the minimum, the first-second quartile boundary (25%), the median (50%), the third-fourth quartile boundary (75%), and the maximum for each distribution.

and AV2 (unstable). Astrophysical parameters were retrieved from the fourth version of the Large Quasar Astrometric Catalog [4] that gathers 443,725 sources including information from the SDSS DR12Q [9] and Gaia DR1 [7].

The parameter-by-parameter analysis is illustrated in Figure 1. The trends observed are that stable sources are fainter in radio, brighter in infra-red, and less observed. Unstable sources are brighter in mag g. No particular trend was observed for the other magnitudes or regarding morphological optical indices. Also, the redshift is not necessarily higher for stable sources. These results are not systematic, as the different candlesticks largely overlap between source categories.

Although interesting, this initial study does not provide help for the identification of the most stable sources. For this purpose, we need to go into further details regarding the relationship between source astrophysics and astrometric instabilities.

3 VLBI Source Position Time Series

We used VLBI source position time series computed in Gattano et al. [3, Section 2]. We only considered 197 sources observed in at least 200 sessions. This number was arbitrarily chosen in consideration of the reduction process. This process aims to filter the high frequency part of the signal presumed to be mainly associated with the observing system.

For each time series, we used a starting window of 32 years and we counted the number of position measurements y_i within it. If greater than 100, we split that window into two half-length windows and proceeded again. When the number of points within a window was between 50 and 100, the average was computed and a new point $\bar{y}_i$ was added to the reduced position time series. If the number of points dropped below 50, the window was ignored. In the end, we obtained reduced time series containing from two to several tens of $\bar{y}_i$ points for each source.

4 Orientation Analysis

Source orientation may be derived in several ways. First, VLBI source images can provide a direction that links two source components if as many are visible. Second, source positions in radio and in optical are sometimes offset in a certain direction. A recent study [10, 6] compared such two directions for thousands of VLBI sources, leading to the conclusion that significant radio-optical offsets favor the jet direction (as revealed by VLBI images) and giving clues as to the existence of an optical jet structure at the parsec scale.

Also, it is possible to extract from our reduced source coordinate time series the direction along which source astrometric instabilities occur, a third direction in the puzzle. To extract the angle θ of this direction, we built the total orientation Probability Density Function [PDF] by considering pairs of successive positions $\left(\overline{\Delta\alpha\cos\delta}_i, \overline{\Delta\delta}_i\right)$ and $\left(\overline{\Delta\alpha\cos\delta}_{i+1}, \overline{\Delta\delta}_{i+1}\right)$ equivalent to vectors (ρ_i, θ_i). Each pair contributed to the PDF by a Gaussian function centered on the orientation θ_i,

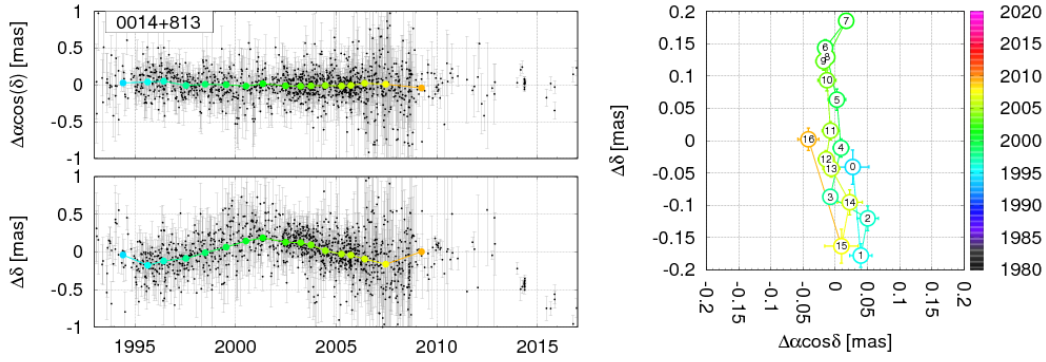

Fig. 2 **(top left)** Position time series of source 0014+813 in black (error bars in gray). The associated reduced time series is given by the colored dots. **(top right)** 2D-representation of the astrometric instability: trajectory drawn from the reduced time series on the local plane centered on the mean position of the source. **(right)** Distribution of the instantaneous directions (from successive positions in the reduced time series). The inset gives the total orientation probability density function in black and its Gaussian fit in red (see Section 4).

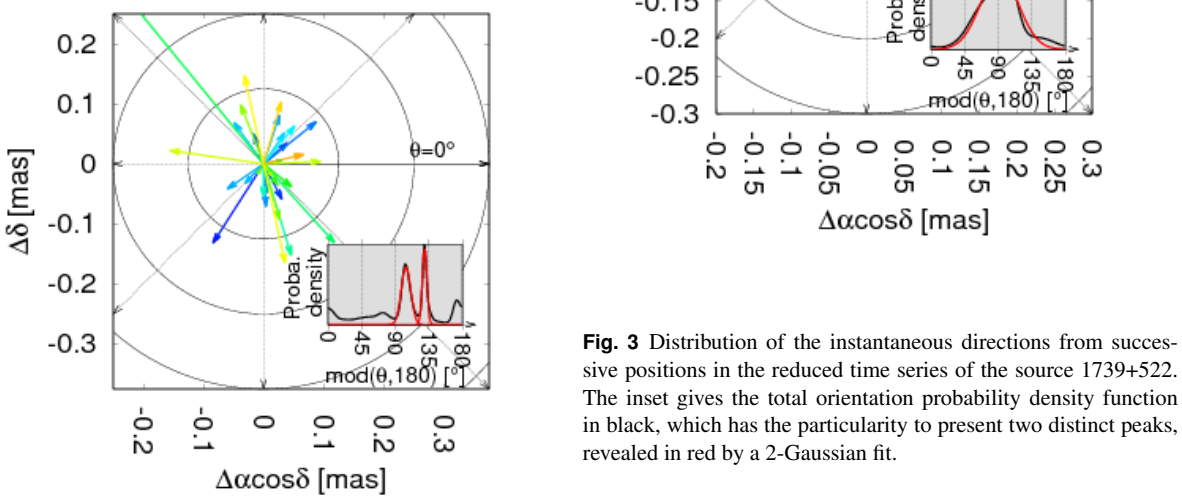

Fig. 3 Distribution of the instantaneous directions from successive positions in the reduced time series of the source 1739+522. The inset gives the total orientation probability density function in black, which has the particularity to present two distinct peaks, revealed in red by a 2-Gaussian fit.

with half-width at half-maximum equal to σ_{θ_i} and an amplitude equal to the ratio between the length ρ_i of the offset and σ_{ρ_i}. The uncertainties σ_{θ_i} and σ_{ρ_i} are computed by error propagation from the coordinates' uncertainties. The built function is finally normalized to respect the property of unit integral.

Then, given this produced orientation PDF, we fitted a global Gaussian function, which provides the preferred orientation θ, its uncertainty σ_θ, and a degree of confidence P_{orient} on θ equal to the integral of the fitted Gaussian function. Figure 2 shows our results for the source 0014+813 ($\theta = 92 \pm 25°$ with 95% of confidence). For some sources, multiple directions can be distinguished. This is the case for the source 1739+522 presented in Figure 3 for which two preferred directions are found : $\theta_A = 105 \pm 6°$ and $\theta_B = 130 \pm 3°$ with 57% of confidence in total.

Results for sources observed in more than 200 sessions are presented in Figure 4. The first plot shows that, with a $P_{orient} \geq 0.8$ threshold, already 60% of the sources have a preferred direction. Secondary orientations appear at $P_{orient} = 0.5$. Approximately 20% of the sources may be subject to a secondary orientation.

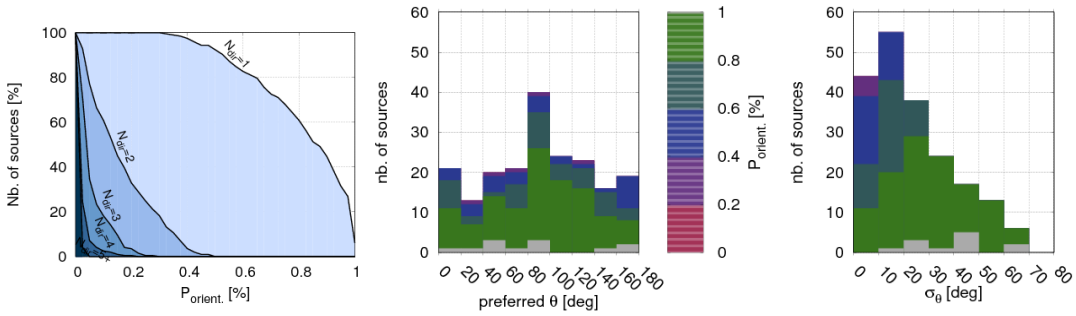

Fig. 4 **(left)** Cumulative histograms of sources with N_{dir} orientations found in the reduced time series as the threshold on the degree of confidence P_{orient} decreases from 1 to 0. **(middle)** Histogram of the source primary orientation found in the reduced time series. The color indicates different intervals of P_{orient}. **(right)** Histogram of the associated uncertainties on the source primary orientation.

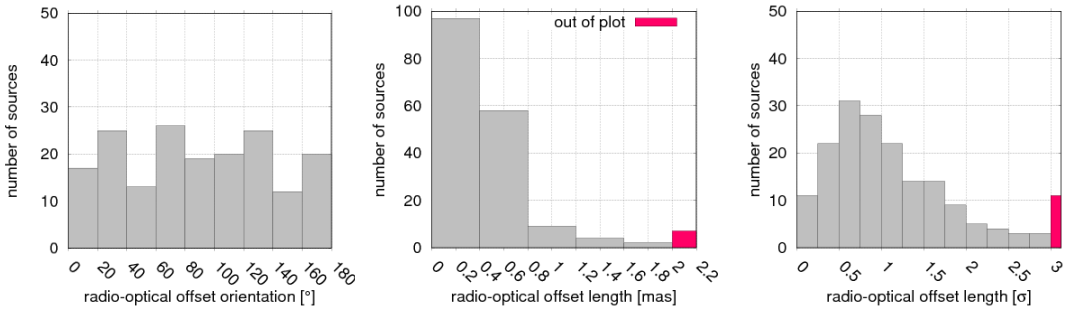

Fig. 5 **(left)** Histogram of the source radio-optical offset orientations. **(middle)** Histogram of lengths in milli-arcseconds. **(right)** Histogram of lengths normalized to the formal errors. The right pink bars also cumulate offsets that are outside the plots.

Nevertheless, the uncertainty on the derived orientation is not so small as seen in the third plot of Figure 4. The distribution peaks at 10–20° and the maximum is greater than 60°. Also, the distribution of the source preferred orientation presents an excess along the declination direction. This is unnatural as sources should be randomly oriented on the celestial sphere. This is probably due to an effect of the observing system, despite the aforementioned low-pass filter.

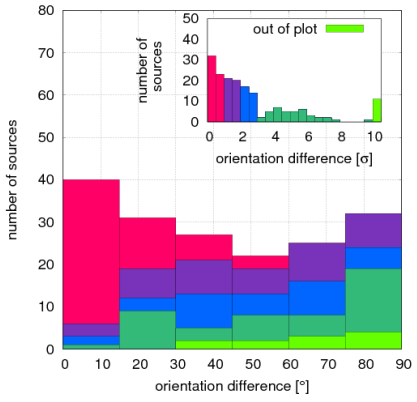

Fig. 6 Comparison between astrometric instability primary directions and radio-optical offset directions. The abscissas give the difference between these two directions in degrees and with respect to the difference uncertainty σ. Each color indicates the level of significance of the direction difference.

In parallel, we focused on the VLBI-Gaia radio-optical offsets. The 2nd data release of Gaia was oriented on a prototype of the ICRF3 [8] thanks to 2,820 VLBI sources with a sufficiently bright optical counterpart. Among the 197 VLBI sources we studied, 177 were found in this subset and we computed their radio-optical offsets. Figure 5 presents the resulting distribution.

The first plot confirms the natural homogeneous distribution of the offset orientations. The distribution with respect to the length shows that most of the offsets are small (more than 50% are less than 0.4 mas). Moreover, only eleven offsets are significant regarding their uncertainty.

5 Comparison and Conclusions

Two astrophysical phenomena may be responsible for the observed radio emission centroid instabilities. First, the source structure may present several components (see for example the Bordeaux Image VLBI Database[1]): one is the main radio core, the others are knots, generally moving along the jet from the main core. The whole configuration of core and knots may be explained by physical process within the jet [5]. Second, the presence of a black hole binary system within the AGN may affect the structure of the source due to two distinct sites of activities. The hypothesis was developed from the mergers between galaxies [1]. Some sources were studied under this hypothesis [12, 2, 11].

Our interpretation of the results is that, when one preferred direction is found for a source, it is probable that the astrometric instabilities follow the evolution of the knot configuration and, therefore, it is aligned with the jet direction. Future comparisons with VLBI images available in the aforementioned database will be useful to test this hypothesis. On the other hand, sources where astrometric instabilities occur along several preferred directions are good candidates for searching binary black hole systems.

Finally, Figure 6 compares the derived directions based on the above mentioned (i.e., from astrometric instabilities) with the radio-optical offsets. Small differences are in general non-significant and characterize a population of sources where those two directions are aligned. If they are also aligned with the jet, the optical centroid is located in the jet. Conversely, sources which show significant differences have values for these differences preferentially near 90°. Hence, if it is the astrometric instability that occurs along the jet, then the radio-optical offset is across the jet and the optical counterpart may be preferably dominated by the accretion disk or the host galaxy. But if it is the radio-optical offset that is aligned with the jet, the astrometric instability occurs across the jet, which is in favor of the search of potential binary black hole.

Adding the source structure orientation from VLBI images to our result will be useful to get further insights into those possibilities.

[1] → http://astrophy.u-bordeaux.fr/BVID/

Acknowledgements

This work was supported by a CNES post-doctoral grant. César Gattano is grateful to the IAG, the CNFGG, and the OASU for supporting the trip and thus allowing the presentation of this work at the IVS General Meeting.

References

1. Begelman, M. C.; Blandford, R. D. & Rees, M. J., Massive black hole binaries in active galactic nuclei, Nature, 1980, 287, 307–309.
2. Britzen, S. et al., On the origin of compact radio sources. The binary black hole model applied to the gamma-bright quasar PKS 0420-014, A&A, 2001, 374, 784–799.
3. Gattano, C.; Lambert, S. B. & Le Bail, K., Extragalactic radio source stability and VLBI celestial reference frame: insights from the Allan standard deviation, A&A, 2018, forthcoming paper.
4. Gattano, C. et al., LQAC-4: Fourth release of the Large Quasar Astrometric Catalogue. Compilation of 443 725 objects including cross-identifications with Gaia DR1, A&A, 2018, 614, A140.
5. Hervet, O. et al., Shocks in relativistic transverse stratified jets. A new paradigm for radio-loud AGN, A&A, 2017, 606, A103.
6. Kovalev, Y. Y.; Petrov, L. & Plavin, A. V., VLBI-Gaia offsets favor parsec-scale jet direction in active galactic nuclei, A&A, 2017, 598, L1.
7. Lindegren, L. and Gaia Collab., Gaia Data Release 1. Astrometry: one billion positions, two million proper motions and parallaxes, A&A, 2016, 595, A4.
8. Lindegren, L. and Gaia Collab., Gaia Data Release 2. The astrometric solution, A&A, 2018, 616, A2.
9. Pris, I. et al., The Sloan Digital Sky Survey Quasar Catalog: Twelfth data release, A&A, 2017, 597, A79.
10. Petrov, L. & Kovalev, Y. Y., On significance of VLBI/Gaia position offsets, MNRAS, 2017, 467, L71–L75.
11. Roland, J. et al., Binary black holes in nuclei of extragalactic radio sources, A&A, 2013, 557, A85.
12. Roos, N.; Kaastra, J. S. & Hummel, C. A., A massive binary black hole in 1928 + 738 ?, Astroph. J., 1993, 409, 130–133.
13. Shabala, S. S. et al., The effects of frequency-dependent quasar variability on the celestial reference frame, J. Geod., 2014, 88, 575–586.